

DEPLOYMENT MECHANISMS ON THE FAST SATELLITE: MAGNETOMETER, RADIAL WIRE, AND AXIAL BOOMS

DAVID PANKOW

Samuel Silver Space Sciences Laboratory, University of California at Berkeley, U.S.A

ROBERT BESUNER

Besuner Consulting Services, Madera, California, U.S.A.

ROBERT WILKES

Lockheed Martin Space Mission Systems & Services, Houston, Texas, U.S.A.

ROBERT ULLRICH

Samuel Silver Space Sciences Laboratory, University of California at Berkeley, U.S.A.

Abstract. The Fast Auroral SnapshoT (FAST) satellite was launched by a Pegasus XL on August 21, 1996. This was the second launch in the NASA SMall EXplorer (SMEX) program. Early in the mission planning the decision was made to have the University of California at Berkeley Space Sciences Laboratory (UCB-SSL) mechanical engineering staff provide all of the spacecraft appendages, in order to meet the short development schedule, and to insure compatibility. This paper describes the design development, testing and on-orbit deployment of these boom systems: the 2 m carbon fiber magnetometer booms, the 58 m tip to tip spin-plane wire booms, and the 7 m dipole axial stiff booms.

Table of Contents

1. Introduction
 - 1.1. Mission Background
 - 1.2. Electric Field Sensor Description
 - 1.3. Spacecraft Dynamics
2. The Magnetometer Mechanisms
 - 2.1. Magnetometer Boom Configuration
 - 2.2. Magnetometer Boom Deployment
 - 2.3. Magnetometer Boom Design
 - 2.4. Magnetometer Boom Testing
3. The Radial Electric Fields Mechanisms
 - 3.1. The Sensors
 - 3.2. Radial Wire Boom Deployment and Configuration
 - 3.3. Deployment Mechanisms
 - 3.4. Wire Boom Testing
4. The Axial Electric Fields Mechanisms
 - 4.1. Design and Configuration
 - 4.2. Testing
 - 4.3. Deployment
5. On-Orbit Performance
6. Summary



Space Science Reviews **98**: 93–111, 2001.

© 2001 Kluwer Academic Publishers. Printed in the Netherlands.

1. Introduction

1.1. MISSION BACKGROUND

The scientific objective of this magnetospheric physics mission was a detailed investigation of the Aurora Borealis, or 'Northern Lights'. The fields experiments (electric and magnetic) were constructed by the University of California at Berkeley (UCB), and Los Angeles (UCLA) respectively. The particles instruments were constructed by UCB and the University of New Hampshire in collaboration with Lockheed Palo Alto Research Laboratory. The instrument data processing unit was provided by UCB. The spacecraft bus, telemetry, and launch services were provided by the NASA Goddard Space Flight Center SMEX office. The science principal investigator is Dr C. W. Carlson of UCB, and the program is managed by the SMEX office.

The UCB design philosophy emphasizes the demonstration of design margins set by peer review. As a result, each boom system was extensively tested at a prototype level before the flight units were manufactured. Additionally, the design, assembly and testing of each boom mechanism was conducted by a single engineer solely responsible for its success.

1.2. ELECTRIC FIELD SENSOR DESCRIPTION

Three orthogonal dipoles with six tip mounted sensors are needed for a vector measurement of the DC and AC electric fields in the plasma. Sounding rocket and early satellite experiments used stiff, deployable booms for the dipoles. Solar-thermal bending and vehicle dynamics severely limited these stiff booms to lengths of several meters, far short of the lengths desired for more precise physical measurements. In the evolution of these instruments, the preferred practical configuration has been found to be a spinning vehicle with four limp wires in the 'spin plane' and two stiff axial booms along the spin axis. The limp wires can be precisely positioned by centripetal acceleration, and are immune to the bending and buckling concerns in stiff booms. These lightweight wires allowed about a tenfold increase in the practical radial boom dipole lengths.

1.3. SPACECRAFT DYNAMICS

In practice, boom lengths are determined by the need for a spin stable vehicle. Briefly stated, a spinning body will be stable about the principal axis having the largest moment of inertia (or second mass moment), based on conservation of angular momentum and body-flexing dissipation of energy by the limp wire to a rotational energy minimum (Meirovitch and Calico, 1972). The spin stability ratio (which must be > 1) is defined as the ratio of the moment of inertia about the spin axis to the larger of the two transverse axes ($I_S/I_{T_{\max}}$), while the stability margin is defined as this ratio minus one. This means the radial wire booms improve stability

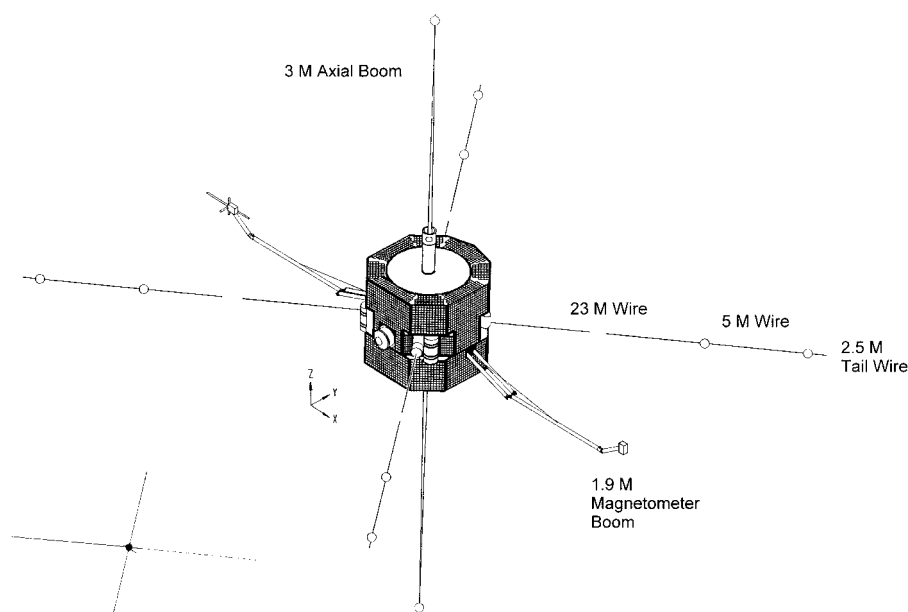


Figure 1. FAST Boom Geometry.

and can be quite long, while the axial booms are length limited because they reduce the stability margin by increasing the transverse moment of inertia.

The wire boom cables are essentially limp: any transient motions or oscillations are induced by spacecraft maneuvers. This pendulum behavior is dependent on the wire root or hinge attachment radius, the distance from the spin axis to the wire attachment (or exit point). On FAST, the radial boom stiffness was enhanced by providing trap doors at the vehicle skin, which increased this hinge radius. There is a practical (spacecraft attitude control system (ACS) stability based) bound on wire length, which is the geometry in which the spin plane torsional resonance equals the spin rate. This mode may be envisioned as a spin plane 'flutter' with all wires swinging in phase and a 180° phase shift for the center body (Lai and Bhavnani, 1975). The FAST boom geometry approached this limit, with a wire boom second mass moment that is 24 times that of the vehicle. The deployed wire boom plane was located close to the spacecraft Z axis center of mass to avoid spin axis tilt caused by wire boom mass moment asymmetries.

The axial booms must be sufficiently rigid to avoid elastic instability and subsequent collapse. As previously stated, the vehicle stability margin limits the boom length. In the mission planning stages, it was decided to include the stabilizing effect of wire booms in the overall moment of inertia calculations, to maximize the allowed axial boom length. In practice this increased the boom length from 2.6 m to 3.8 m each, which is a very significant improvement for minimizing the effects of vehicle photo-electron emission. Conventional wisdom would suggest that boom length might be increased by decreasing the boom mass, which will also

decrease the stiffness. However, spin induced boom flexing amplifies the 'effective' boom second mass moment (Meirovitch and Calico, 1972). A boom cantilever resonance of four times the spin (as compared to a customary requirement of two) was selected to maximize boom length.

A systems issue is evaluation of the spin axis alignment budget. A list of many uncertainties, ranging from deployed boom straightness to alignment of the vehicle balance fixtures, will affect the alignment of the spin axis with the vehicle geometric axis. Simple addition of this list is far too conservative, and not warranted. If each of the uncertainties is assumed to have random clocking with respect to the spin axis, the resulting imbalance is one half the root square summation (RSS) of these residual inertia products. The traditional minimum requirement for the vehicle stability margin is 4%, based mostly in the uncertainties of mass moment measurements. Sensitivity of the spin axis alignment indicated that a more practical stability minimum was 8–10% for this satellite.

1.4. BOOM DEPLOYMENT SEQUENCE

The deployment sequence for FAST released the magnetometer booms, the radial wire booms, then the axial booms. For both enhanced reliability and simplicity, these boom mechanisms are purposely designed without a retraction capability. The boom systems are manually rewound and reset after ground testing, and on-orbit retraction is neither possible nor necessary.

2. The Magnetometer Mechanisms

2.1. THE MAGNETOMETER BOOM CONFIGURATION

System constraints imposed on the magnetometer booms were straightforward. They must be stiff compared to the other booms (to avoid dynamic interactions) and thermally stable to maintain alignment of the sensors. A two meter separation from the spacecraft was determined to be adequate to avoid the false signals related to spacecraft current loops and digital circuitry. Perhaps the greatest challenge in the design of these booms was fitting within the 50 mm irregular annulus between the solar array and the launch vehicle fairing.

Fluxgate, search coil, and attitude control system (ACS) magnetometers are installed on two deployable, articulated, carbon-fiber booms, approximately two meters in length. Significant features of the magnetometer booms include latchless hinges, low mass, and an innovative carbon-fiber/epoxy fabrication technique.

Each magnetometer boom assembly consists of a base assembly, dual inner boom segments, an outer boom segment, and saddles at the upper and lower corners of the spacecraft solar arrays. The base assembly includes a centrifugal brake to control deployment velocities, a restraint/deployment assist system, electrical

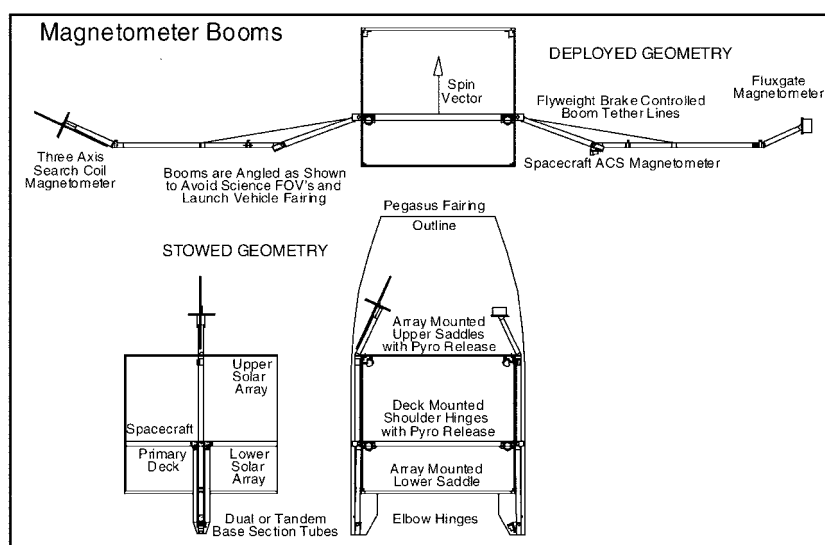


Figure 2. Magnetometer Boom Configuration.

connectors for spacecraft ‘housekeeping’ and magnetometer data, and the ‘shoulder hinge’. The inner boom segment is composed of two carbon-fiber tubes, side by side, with space between them in which the outer boom segment nests. The outer boom segment is hinged to the inner segment and is comprised of carbon-fiber tubes with aluminum ‘hard points’ where the boom is restrained for launch dynamics. The outer boom elements are angled to clear the launch fairing of the Pegasus XL. The science magnetometers (fluxgate and search coils) are mounted at the ends of the booms. The ACS magnetometer is located on the elbow hinge of the fluxgate magnetometer boom.

The booms are mounted to the deck on opposite sides of the spacecraft. During launch, the booms were stowed against saddles on the sides of the spacecraft solar arrays, restrained by stainless steel cables at the spacecraft deck and by beryllium-copper rods at the upper array corners. The booms were preloaded against the deck and solar array edges to reduce the launch induced vibration amplitudes. This three-point bending geometry bowed the middle of the booms toward the spacecraft with a force at the deck of ~ 450 N. High force, short travel spring based deployment assist plungers were incorporated in the deck mounts, to overcome any binding forces that might develop in the mounts. These plungers also freed the centrifugal brakes, which were locked by the plungers for launch.

2.2. MAGNETOMETER BOOM DEPLOYMENT

Once the spacecraft was in orbit and spinning at 20 rpm, the magnetometer booms were deployed by firing pyrotechnic cable cutters at the upper saddles and shoulder hinges. Centrifugal force motivated the deployment. The speed of deployment was

controlled by a tether attached to the outer boom segment which spun a centrifugal (flyweight) brake in the base hinge assembly. The function of this brake is to provide a force balanced boom deployment environment, so that the booms could be deployed over a wide range of spin rates. Analysis and test set this range to be 12 to 60 rpm. The final deployed position of the booms was determined by hard stops in the hinges. These hard stops consist of v-blocks into which the round boom nests. There is no latching mechanism. The position along the spin (Z) axis of the line of force due to centripetal acceleration of each boom / magnetometer assembly is between the Z positions of the shoulder and elbow hinges. This causes the shoulder hinge to try to rotate in the spacecraft up direction and the elbow hinge to try to rotate in the spacecraft down direction, into their respective V-block stops. Torsion springs in each hinge assured deployment and increased loads on the stops. The normal spring end and coil forces push each hinge pin against its clevis holes to prevent hinge rattle.

2.3. MAGNETOMETER BOOM DESIGN

Carbon fiber/epoxy was chosen as the primary structure of the booms due mainly to its very high stiffness and strength to weight ratio, as well as the low thermal expansion coefficient. The magnetometer signal and power wires were routed inside the boom tubes and hinges using coaxial cables. Each boom also included an outboard connector, so that the magnetometers could easily be removed for testing. Harnessing was reduced to about 40% of the customary weight by using Goretex dielectric and helically served foil coaxial shields with six drain wires. Served shield coax is not only lighter and more flexible than the braided shield option, but also provides better electrical coverage. In spite of these weight saving measures in the electrical harness, it was still 25% heavier than the composite boom tubes. The total mass of the two booms, including the restraint mechanisms, saddles, tubes, balancing mass, and interfaces to the magnetometers is 3.5 kg. The total mass of the three magnetometers is 1.8 kg.

The carbon fiber/epoxy tubes were constructed from 5 layers of woven prepreg material. The 0.14 mm thick layers were laid out with $0^\circ/90^\circ$ orientation for the outer, inner, and middle layers, and $\pm 45^\circ$ orientation for the two mid-layers. The finished tubes have an outside diameter of 32 mm and a wall thickness of 0.7 mm. The tubes were fabricated by SSL personnel in the Composite Materials Laboratory of the UC Berkeley Mechanical Engineering Department, directed by Prof. Hari Dharan. The epoxy pre-impregnated material was laid by hand on a polished aluminum mandrel, then wrapped with a film of PTFE Teflon. Instead of using an autoclave or vacuum bagging, a length of thick-walled neoprene heat shrink tube was placed around the uncured tube. The shrink temperature of the tubing is the same as the cure temperature of the epoxy in the prepreg (175°C). The entire assembly was baked for two hours and cooled. The shrink tube was carefully sliced off, and the aluminum mandrel thermally contracted to release the finished tube.

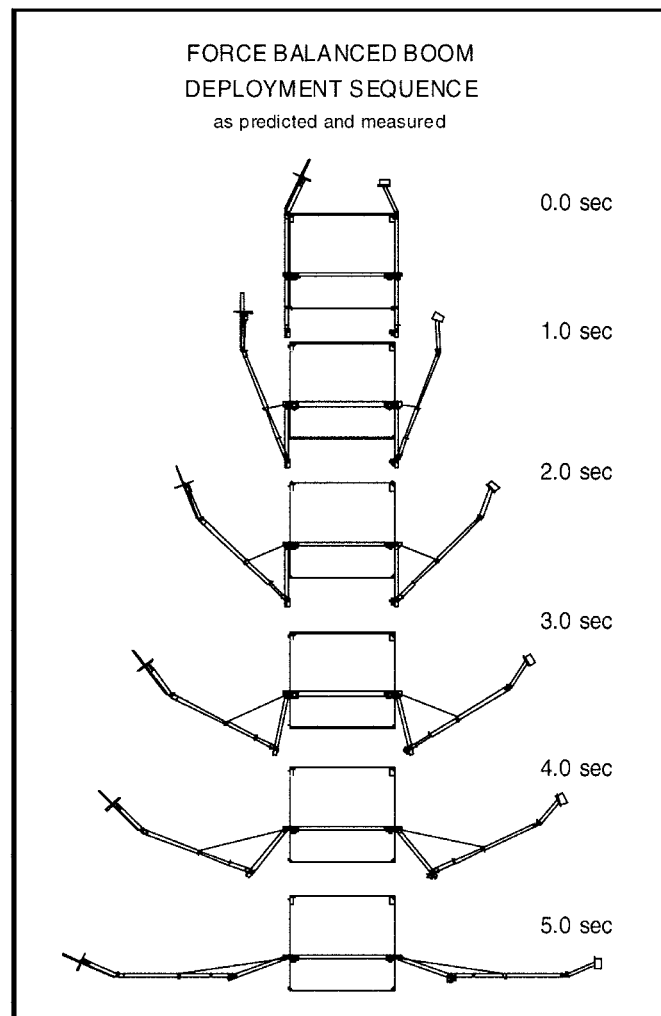


Figure 3. Magnetometer Boom Deployment.

Avoiding the use of vacuum bags or autoclaves significantly reduced labor and expense and produced uniform, high quality tubes. The metal to composite tube joints used thin aluminum sleeves bonded with structural epoxy (both internal and external) to minimize both distortions and stress concentrations. Alternating bands of aluminum tape and conductive black tape were chosen by the SMEX office for the thermal control, so as to minimize the temperature excursions in shadow.

2.4. MAGNETOMETER BOOM TESTING

Testing of the boom systems included vibration and deployment testing. Deployment tests were conducted in two configurations: ceiling drops and spin tests.

For ceiling drop tests, a boom with magnetometer mass dummy was installed on a fixture simulating the side of the spacecraft mounted to the ceiling of the test facility. The fixture was tilted about the spin axis to approximate tangential coriolis accelerations of the actual deployment. The boom was released, and the boom segment relative angles were measured using potentiometers at the hinges. Overload tests were conducted using oversized instrument mass dummies. Spin tests were conducted on a spin table with a fixture simulating two sides of the spacecraft. Also mounted to the table was an overhead track on which rode trolleys carrying constant-force springs. The springs were fastened to key points on the magnetometer booms to counter the effects of gravity. The table was spun at various speeds, and the booms were deployed to verify computer simulations. Numerical prediction of the deployment environment was a vital part of the design process, to establish the needed strength and stiffness margins.

Deployment testing and flight deployments showed that the final position of the magnetometers were repeatable to ~ 1 mm, while the science magnetometer orientation was repeatable to ~ 3 arc min, and deployed boom resonance was above 2 Hz. The unequal weights of the three magnetometers led to concerns of spacecraft balance. Balance weights were added such that that the spacecraft was dynamically balanced with the booms removed, or deployed. As a result, FAST was launched with an intentional one degree tilt of the spin axis, which went to zero when the booms were deployed shortly after separation.

3. The Radial Electric Field Mechanisms

3.1. THE SENSORS

The primary sensing elements for the FAST vector electric fields experiment are ten 8 cm spherical sensors. Each axial boom has one sensor, while each of the four 30 m wire booms has two sensors separated by five meters. Each of the sensors contains a pre-amplifier which uses a variety of active feedback schemes to achieve an ultra-high impedance measurement of the local plasma potential, while also minimizing the local disturbances of the plasma. The preamps are housed in 1 mm thick aluminum shells, which are coated with electrically conductive DAG-213 (an epoxy based paint doped with fine carbon particles).

The $\varnothing 2.5$ mm electrical cable used for wire booms is of an advanced construction, designed at UCB/SSL and fabricated by W.L.Gore, Inc. This cable includes two $\varnothing 0.6$ mm fifty Ohm coax cables and eight AWG #36 conductors. The central wire bundle is jacketed with a Kevlar braid, an aluminized Kapton conductive foil, and a silver plated copper outer braid. With Kevlar as the internal strength member of the cable, we were able to cut and electrically isolate the outer braid, as desired. In fact, each boom cable is divided into eight surfaces that are electrically biased, so as to minimize the disturbances of the conductors and spacecraft in the local

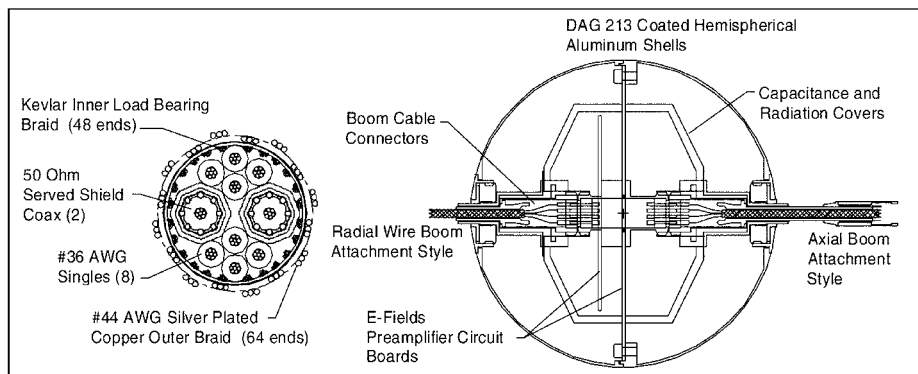


Figure 4. Wire Boom Cable (20 \times) and Electric Fields Spherical Sensor.

plasma. Special attention to design and fabrication details ultimately provided a very flexible cable, which was shown to deviate less than 10 mm from the desired limp wire radial line. One of the formidable engineering tasks was to also produce a very low thermal expansion cable, so as to avoid ‘wind-up’ effects of the rapidly cooled and reheated cable each time the satellite traverses the earth’s shadow. The Kevlar braiding could not alone provide the desired low expansion cable. We utilize the fact that the cable core is mostly Teflon insulation (by volume) covered with a helical wrap. This results in an apparent negative expansion as the helical path length increases (when the cable warms in sunlight) due to an expanding Teflon core diameter. The sphere connectors provide a ‘plug & play’ design, wherein any of the cables, sensors, or preamps could be rapidly swapped out (as needed) without mechanism tear down or cable de-soldering. The $\varnothing 10$ mm \times 15 mm miniature boom cable connectors for each cable end were also a custom UCB design using developmental pins and sockets provided by Hypertronics, Inc.

A major boom mechanism design challenge was the proper handling of the spheres. Since the painted surfaces of the spheres are the primary science sensing surfaces, blemishes or abrasions simply could not be tolerated. No contact of the sphere surface could occur during ground handling, launch, or deployment. Small $\varnothing 4$ mm stubs protrude from either side of each sphere, and these were used to support the sensors.

3.2. RADIAL WIRE BOOM DEPLOYMENT AND CONFIGURATION

Each radial wire boom has two spherical sensors and three cable assemblies; a 23 m inner cable, a 5 m sphere to sphere cable, and a 2.5 m ‘tail wire’ (extending beyond the outer sphere to provide electrical, thermal and mechanical symmetry about the sensor).

A mechanism design issue was the on-orbit activities needed to deploy this rather complex wire geometry, without impacting the delicate body mounted solar array, touching the surfaces of the spheres, or tangling the cables on the magne-

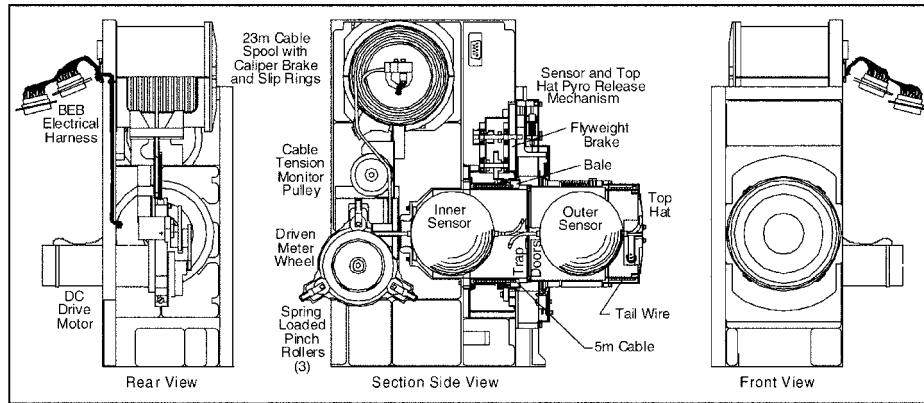


Figure 5. Wire Boom Deployment Mechanism.

tometer booms. The deployment of the wire boom was broken up into three events corresponding to each cable assembly. The three cable assemblies were deployed by a different method.

3.2.1. 5 m Cable Deployment

The outer sphere and a protective ‘Top Hat’ were released by the firing of a pyro, and pulled outward by an initial centripetal acceleration of 0.3 G. The centripetal acceleration varies as the outer sphere travels away from the spacecraft, and increased to over 1.5 G. This first deployment of a pair of booms also slowed the spin of the spacecraft from 25 to 17 rpm, within approximately 60 s. A centrifugal brake on the deploying cable limited the cable feed rate to below 0.08 m s^{-1} , in order to keep the coriolis induced wire boom offsets to less than 10° from true radial, well away from the magnetometer booms, which are at 45° from the wire booms.

3.2.2. Tail Wire Deployment

After an opposed pair of 5 m sphere to sphere cables were deployed, the spacecraft was spun back up to 25 rpm to release the Top Hats. The Top Hats were held to the outer sphere by a force latch that released at $\sim 2 \text{ G}$'s. Release of the Top Hats rapidly unfurled the $2\frac{1}{2} \text{ m}$ tail wire, well away from the spacecraft. The Top Hats were discarded.

3.2.3. 23 m Cable Deployment

With the outer sensors and cables deployed, the wire booms were ready for the third event, metered deployment of the 23 m main cable. On orbit, this stage was done in two meter increments, with constant ACS spin-up torqueing, in order to maintain a minimum 12 rpm spin for continuous science data.

3.3. DEPLOYMENT MECHANISMS

3.3.1. *Top Hat Release*

For launch, the inner sphere was housed inside a spool within the body of the boom mechanism. The outer sphere was housed in the Top Hat, which was held against the boom housing by four latches. The outer $2\frac{1}{2}$ m tail wire was wrapped into an annulus in the Top Hat. A $\varnothing 0.61$ mm hat retention cable circled the Top Hat, and held the latches against the Top Hat with a noose-like action. The cable circle changes diameter, and correspondingly drives in or releases the latches, with the position of a tension arm. The tension arm position was also used to simultaneously lock and unlock the centrifugal brake mechanism. The tension in the hat retention cable was maintained with a pair of redundant springs, which were tied to the tension arm by a pair of $\varnothing 0.46$ mm cables. Release of the Top Hat and flyweight brake occurred with the firing of a pair of redundant pyro operated cable cutters, each of which severed the pair of $\varnothing 0.46$ mm cables, freeing the tension arm, allowing the hat retention cable circle to expand, thereby releasing the latches. Confirmation of Top Hat release is provided by a microswitch acting directly on the edge of the Hat. The pyrotechnics are ICI Americas type 192Y subminiature wire cutters. They are $\varnothing 4.8$ mm \times 27 mm and contain a 25 mg explosive charge.

3.3.2. *5 m Cable Payout*

The sphere stubs between sensors were supported by a pair of spring loaded trap doors. The 5 m sphere to sphere cable was routed to the exterior of the spool, and wrapped into an annulus around it. The cable was held in place simply by fixing the cable endpoints. A rotating 'bale' that will later allow the cable to peel out from the end of the spool, one coil at a time, lay at the external edge of the spool. This bale operation is analogous to, but opposite of, the bale on a spin casting fishing reel. In the wire boom, a rotation of the bale is required to remove cable from the spool, with the fishing reel, the bale rotation acts to wind fishing line onto the reel. The bale is linked to a centrifugal (flyweight) brake through a 20:1 step up gear train, to control the speed of cable pay out. The flyweight brake uses spring loaded PEEK friction pads, acting against an aluminum housing. The entire gear train is supported by Barden dry film lubricated ball bearings. No preload of the bearings can be tolerated, as the bale must function with only a 5 g tangential input. All gear and bearing spacing requirements are therefore controlled by shims. This was the most critical aspect of the mechanism, as even a light preload from wavy washers caused undetected imperfections or perhaps dry film particulate in the bearings to produce unacceptable spikes in the rotating torque. The brake mechanism maintains a payout speed of $0.06\text{--}0.08$ m s⁻¹, despite variations in the wire tension of over a factor of 5.

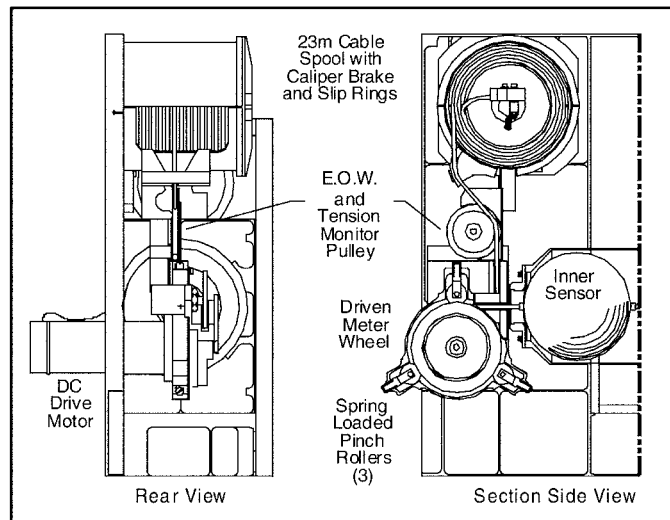


Figure 6. Spool Mechanism Detail.

3.3.3. 2.5 m Cable Payout

The release of the Top Hat by the latches freed the Hat, which contains a spring loaded Acetal (Delrin) sleeve. This sleeve pushed the Top Hat away from the spacecraft, and simultaneously opened the end of the annulus containing the 2.5 m cable. Constraint of this cable is required for launch, and the sleeve motion allowed it to peel out of the annulus freely, upon separation of the sphere from the Top Hat. The force latch which controlled the separation of the sphere from the Top Hat consists of a torsion spring acting on an arm, which engaged the sphere stub through a small hole in the stub. The preload of the torsion spring was set such that a 2 G load on the Top Hat will allow the arm to rotate, which released the sphere.

3.3.4. 23 m Cable Payout

The 23 m cable deployment mechanism (see Figure 6) contains a rotating cable storage spool, a metering wheel cable deployment assembly, a vacuum-service brush DC gear motor, over-tension and end-of-wire (E.O.W.) indicators, analog and digital cable length indicators and redundant gold alloy slip ring electrical contacts on the inboard end. The mechanism deploys cable at a nominal rate of 8 mm s^{-1} with tension ranging from 0 to 100 N. The drive motor is magnetically and EMI shielded. The meter wheel cable grip is enhanced by three equally spaced spring loaded pinch rollers. The meter wheel and pinch rollers have fluorocarbon (Viton) surfaces to avoid damaging the cable braid. The internal cable over-tension indicator prevents breaking and ‘discarding’ the cable, should a motor malfunction occur.

3.4. WIRE BOOM TESTING

Both horizontal and vertical deployments were used to test the wire boom deployment, most testing being focused on the dynamics of the 5 m cable segment. Vertical deployments downward were used with varying masses at the sphere/Top Hat location to verify margins and to allow 3-dimensional dynamics. Deployment was demonstrated with masses of 39, 119, 350, 606, 2270 and 3180 g. This demonstrates a 0.11 to 9 G range, simulating a range of spacecraft rpm of 15–135. The predicted 8° coriolis angle was simulated by tilting the boom housing during these deployments.

Horizontal tests both in air and in thermal vacuum were conducted by constraining the sphere/Top Hat to a linear track, and allowing the boom to pivot freely about its center of gravity. This only provides one plane of motion for the deployment dynamics, but was sufficient for acceptance testing of the flight units, allowing operation through the range of -40°C to $+60^\circ\text{C}$ to be demonstrated. All horizontal testing employed a continuously variable clutch to provide a tensile force on the Top Hat in place of the centripetal force. This force could be changed during the deployment to match the force profile that would be encountered on orbit, but in practice, the lowest level initial force was retained throughout the deployment as a worst case. The subsequent spin up and Top Hat separation force were verified by increasing the tensile force on the Top Hat with the variable clutch until separation occurred.

Each boom was deployed horizontally after 3 axis vibration testing, and after thermal/vacuum cycling.

4. The Axial Electric Field Mechanisms

4.1. DESIGN AND CONFIGURATION

The axial booms consist of the boom element (Stacer), guiding and stiffening nozzles, a deployment assistance device (DAD), spherical sensor with electric field biasing elements, and a carbon-fiber housing.

4.2. STACER

The FAST spin axis sensors use a boom commercially known as a ‘Stacer’, a proprietary device developed by the Hunter Spring Co, and now owned by Ametek. The boom is a rolled strip material of spiral-wound, fixed-helix angle that forms a gently tapered hollow tube when deployed. In its stowed state, it fits within a short cylinder. This boom geometry resembles the ‘Chinese yo-yo’ sometimes used as birthday party favors.

The Stacer element is cold formed using 0.12 mm thick \times 126 mm wide Elgiloy strip material. The strip is formed with a constant (fixed) free coil diameter and

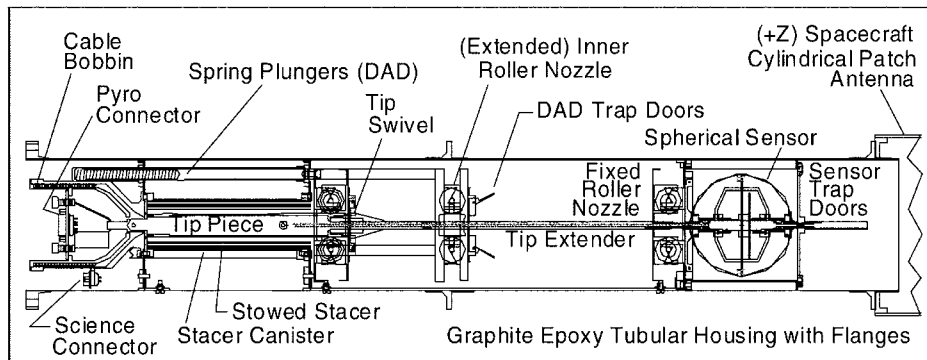


Figure 7. Stowed Axial Boom (section view).

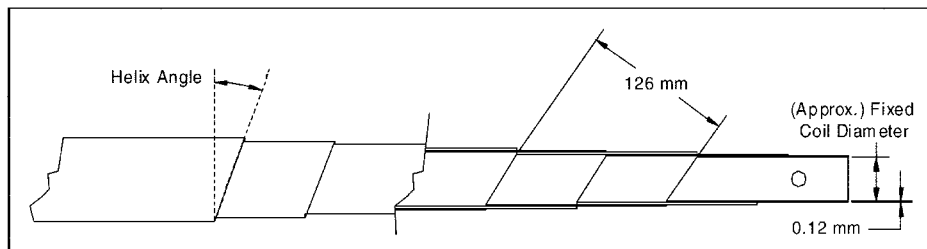


Figure 8. Stacer Detail.

helix angle. The preferred forming geometry involves significant coil overlap, such that two layers of strip material would be found at any point along the length of the extended Stacer element. The deployed end inner-most coil cinches on a cylindrical tip piece and the subsequent coils of an extended boom element 'stack' on the previous coils producing the characteristic taper. Typical deployed coil diameters are slightly larger than the free coil diameter, which means that normal forces exist between coils due to this 'stacking' process. These intercoil forces in turn produce intercoil friction forces that prevent gross coil slippage. The resulting boom has bending stiffness and strength which compare favorably with the equivalent solid thin walled tube.

A primary advantage of the Stacer element, as compared to other stiff boom geometries, is its thermal symmetry. The usual alternative uses two longitudinal cambered ($>180^\circ$) strips that overlap lengthwise to form a tube. The low thermal conduction between strips can produce significant thermal bowing (Staugaitis and Predmore, 1973), which has been known to cause thermal pumping on slow spinning spacecraft. The helical overlap of the single Stacer strip, by contrast, is axi-symmetric for circumferential heat flow. Other advantages of the Stacer are that it does not need a motor driven deploy mechanism, and the fact that a cable may easily be fed up the center of the boom.

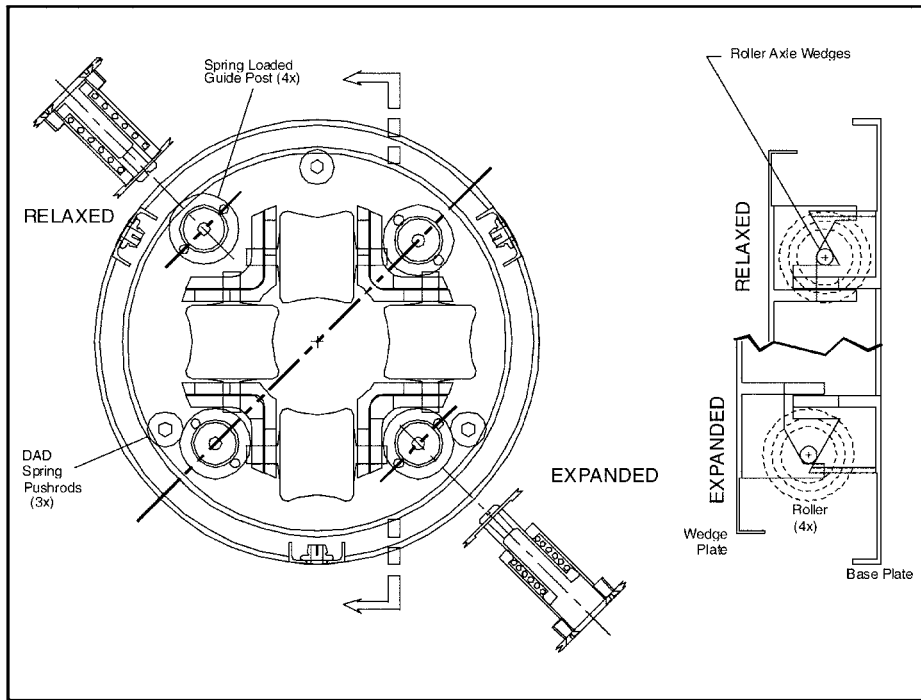


Figure 9. Axial Boom Roller Nozzle Detail.

4.2.1. Boom Support Nozzles

Two roller nozzles were used to give the axial boom the required cantilever stiffness. They were positioned beyond the Stacer canister: one attached to the deployment assistance device mounted on the canister itself, and the other mounted on the end of the main carbon fiber housing. This design maximized the separation between the nozzles to provide a rigid pinned-pinned base support.

The expanding roller nozzle design was developed to accommodate the changing boom diameter, while also minimizing friction. Axles of the four rollers are held between the base and wedge plates by spring loaded guide posts. The resulting geometry allows concentric outward movement of all rollers, but produces a friction lock when only one roller is loaded by cantilever boom bending, thus providing a centering force. The boom element thus has full cantilever stiffness.

4.2.2. Deployment Assistance Device (DAD)

The inner roller nozzle was held against the canister for launch by trap doors that caught the edge of the Stacer tip piece, and was then pushed beyond the coil transition zone by spring loaded plungers when the boom was released. These plungers also provided an initial kick force to help the 'cinching' of the first coil on the tip piece, and a robust deployment of the remaining coils. After the pyro initiated release, the DAD plunger pushed the tip piece to beyond the coil forming zone of

the Stacer, and then the trap doors were pushed open by the deploying boom. Once the boom was mostly deployed, the rollers were contacted, and limited the booms range of motion to its axial component.

4.2.3. *Electric Field Biasing Elements*

As mentioned before, the best e-field measurements can be made if the photo-emissions from the space craft and the boom mechanisms can be nullified. The axial booms used stiff stubs that were insulated from the main spherical sensor and the Stacer by PEEK plastic. Thin-walled aluminum tubes: $\varnothing 6 \text{ mm} \times 250 \text{ mm}$ long were used for these stubs, coated with the same DAG 213 as the sensors. These provided the electrically bias able inner 'stub' segments. A shorter piece of the same material was mounted to the exterior of the sensor, for symmetry.

A UCB design electrical connector between sensor and stub allowed swapping of the sensors without disturbing the boom. This assembly was then attached to the Stacer tip piece, utilizing a rotating sleeve in a collar that allows the Stacer to deploy without causing the sensor cable to twist. The edge of the collar projected to form a lip for the DAD trap doors to catch.

The axial boom electrical cable was stored for launch on a bobbin below the boom canister. The bobbin annulus was sized to prevent crossing and subsequent tangling of the cable coils. The cable was pulled from the end of the bobbin, drawn up the center of the boom element as it deployed, and also aided in stopping the element at its desired final length. A microswitch was positioned to record the unwinding of each coil as it was pulled off the bobbin, giving length and sensor velocity measurements.

4.2.4. *Carbon Fiber Housing*

The entire axial boom mechanism was secured to the FAST spacecraft inside carbon fiber housings, one each for $+Z$ and $-Z$ axes. These housings were built on the UCB campus in the Composites Lab alongside the magnetometer booms.

Each boom assembly is mounted in a $\varnothing 100 \text{ mm}$ thin wall graphite/epoxy tube. The tube consisted of 5 layers of a Fiberite 0.14 mm thick prepreg woven carbon material. The inner, middle and outer layers were laid-up at $0^\circ/90^\circ$ while the layers between were set to $\pm 45^\circ$. They were laid up on a polished aluminum mandrel, covered with perforated Teflon release material, bleeder batting and vacuum bagged before curing. After curing, the thermal contraction of the aluminum mandrel as it cooled allowed the tube to slip free. The lower tube was 670 mm long, the upper tube was extended to 800 mm in order to support the S-band antenna well away from spacecraft. After light bead-blasting to remove the insulating epoxy surface, flanges were epoxied to the outside of the tube to provide mounting points for thermal blankets, the antenna and the flange to bolt the boom to the S/C deck. This bead-blasting also allowed the tube to meet electro-static cleanliness requirements without further processing, by exposing the carbon fibers.

4.3. AXIAL BOOM TESTING

The testing of the axial booms utilized 2 methods of deployment. Initially the boom was deployed vertically upward to yield an unbiased-by-gravity concentricity/target accuracy measurement. The unit was mounted coaxially on a spin-table base, and after deployment, the unit was spun and the total indicated run out (TIR) was measured. The axial boom was then deployed horizontally with the tip piece attached to a low friction trolley on a track. This allowed the Stacer to develop full speed, which gave full length, and therefore allowed a very accurate measurement of deployed length. The deployment microswitch state-changes were measured for all deployments and compared. 3 axis non-combined vibration tests were run, after which the booms received 4 hot/cold cycles of thermal vacuum. The horizontal deployment rig was also used in thermal vacuum testing: after hot/cold soaking, each boom was deployed down the trolley track in a 'snout' attached to the chamber. One boom was deployed hot (+50 °C), the other cold (-35 °C). After inspection, a final verification deployment was done. Final inspection and stowing for launch completed the axial booms.

Deployed boom straightness was found to be the order of ± 1 cm at its 3.8 m length, and the cantilever resonance was above 1 Hz. In this free-pop configuration, the extension velocity reached ~ 6 m per second. As such, it was prudent to include some form of extension restraint in order to reduce the shock forces at the end of the extension stroke. This was achieved by sheathing the last bobbin coil with PTFE shrink tube. The tight fit within the bobbin annulus provided the needed retarding force as the boom reached full length. Without the retarding force, there exists a chance that the boom momentum could tear out the retaining rivet, causing a 'floppy' boom.

4.4. DEPLOYMENT

Prior to deployment, the Stacer element was elastically compressed into the canister whose length is only the strip width. The DAD was also compressed, and the two sets of trap doors placed in their launch positions. The outboard passive 'trap doors' supported the sphere for launch. The sensor cable was then wound around the bobbin, and carefully slid into its housing. Last, the pyro assembly was installed and tensioned. The boom was restrained by a 'fishhook' geometry on the rear of the tip piece. This hook was held with an aircraft cable loop that was cut by pyro activated cable cutters to release the boom.

Upon signal from the ground, the pyro ignited, and cut the wire. The Stacer then rapidly self extended by its spring energy as a one shot device, aided by the DAD. The spring force is due to the release of strain energy as the larger diameter stowed coils 'collapse' onto the previously formed boom coils within a single coil transition zone. At full extension, the boom was positioned by the 2 roller nozzles resting tightly against the Stacer element.

5. On Orbit Performance

The FAST spacecraft was launched on a Pegasus XL on August 21, 1996. Within one week, the spacecraft was turned on, and the magnetometer booms deployed at a spin rate of 20 rpm. After a spin up to 25 rpm, the deployment sequence was begun on the first pair of wire booms.

One of this first pair of wire booms, boom #2, stopped after 25 cm of deployment, the other deployed out to 5 m. In an attempt to free the stuck boom and to release the Top Hat from the sphere, the spacecraft was spun up to 40 rpm. Subsequently, the spacecraft was slowed down, then 'kicked' with the highest impulse available with the torque coil. None of these maneuvers were able to move the boom any farther out. The second pair of wire booms were then deployed, both extending to 5 m. Top Hat separation occurred during the 5 m deployment.

The three booms that deployed to 5 m were then extended out to their full 23 m length. Because the booms deployed from slightly below the CG of the spacecraft, the asymmetric load due to the partially deployed boom caused the spacecraft to tilt. Deployment of the +Z axis axial boom shifted the spacecraft CG upward, which decreased the tilt. Because deployment of the -Z axis boom would shift the CG farther below the plane of the wire booms, it was decided not to deploy this boom.

The on orbit deployment failure in wire boom #2, most likely due to the 5 m cable crossing over itself during launch, was unfortunate. The location of this boom during the horizontal Pegasus launch was down, superimposing a DC acceleration during the launch and pull-up which would tend to bias any cable motion to the edge of the Spool, where the possible cable crossover would have occurred.

This has moved the composite center of mass ~ 5 cm from the spacecraft axis, causing the two adjacent wires to shift 6° in the spin plane, toward the missing boom. This somewhat triangular wire boom orientation still provides excellent planar components of the vector fields measurement. The vehicle spin axis has only a 0.4° tilt from the geometric axis, well within the established science tolerances. This is also flight verification of the widely held opinion that vehicle dynamic balance takes precedence over the static balance.

The unprecedented science data obtained is a tribute to the robust nature of this system architecture. On orbit, the FAST vehicle has been found to have excellent attitude stability and spin axis maneuverability. Eclipse spin up, caused by rapidly cooling wires, has been found to be only one part in several thousand. The 'negative orbit normal cartwheel' orientation of spin to orbit makes the vehicle relatively immune to gravity gradient disturbances.

6. Summary

The FAST boom mechanisms designs have evolved over a period of twenty years, from a series of successful satellite instruments flown on S3-3, ISEE, Viking, Freja, CRRES, Polar, and Cluster 1 and 2. This FAST mission was a unique opportunity to advance the state of the art of the three boom systems it employed. It was predicated as a higher risk mission with a short development and fabrication cycle. The spacecraft subsequently achieved its science objectives, and by doing so, provided engineering development history for future missions to call upon.

Acknowledgments

Dr. Charles Carlson, University of California Berkeley is Principle Investigator for the FAST Mission.

References

- Lai, S. T. and Bhavnani, K. H.: *Dynamics of Satellite Wire Boom Systems*, AFCRL-TR-75-0220.
Meirovitch, L. and Calico, R. E.: 1972, *The Stability of Motion of Satellites with Flexible Appendages*, NASA CR-1978.
Staugaitis, C. L. and Predmore, R. E.: 1973, *Thermal Static Bending of Deployable Interlocked Booms*, NASA TN D-7243.
Thomson, W. T.: 1961, *Introduction to Space Dynamics*, J. Wiley, New York.